The Journal of Immunology

Early Induction of Polyfunctional Simian Immunodeficiency Virus (SIV)-Specific T Lymphocytes and Rapid Disappearance of SIV from Lymph Nodes of Sooty Mangabeys during Primary Infection

Mareike Meythaler, Zichun Wang, Amanda Martinot, Sarah Pryputniewicz, Melissa Kasheta, Harold M. McClure, Shawn P. O'Neil and Amitinder Kaur

J Immunol 2011; 186:5151-5161; Prepublished online 25 March 2011;
doi: 10.4049/jimmunol.1004110
http://www.jimmunol.org/content/186/9/5151

The Journal of Immunology is published twice each month by
The American Association of Immunologists, Inc.,
1451 Rockville Pike, Suite 650, Rockville, MD 20852

Print ISSN: 0022-1767 Online ISSN: 1550-6606.

Early Induction of Polyfunctional Simian Immunodeficiency Virus (SIV)-Specific T Lymphocytes and Rapid Disappearance of SIV from Lymph Nodes of Sooty Mangabeys during Primary Infection

Mareike Meythaler,* Zichun Wang,*,[1] Amanda Martinot,[†] Sarah Pryputniewicz,* Melissa Kasheta,* Harold M. McClure,[‡,2] Shawn P. O'Neil,[†,3] and Amitinder Kaur*

Although the cellular immune response is essential for controlling SIV replication in Asian macaques, its role in maintaining nonpathogenic SIV infection in natural hosts such as sooty mangabeys (SM) remains to be defined. We have previously shown that similar to rhesus macaques (RM), SM are able to mount a T lymphocyte response against SIV infection. To investigate early control of SIV replication in natural hosts, we performed a detailed characterization of SIV-specific cellular immunity and viral control in the first 6 mo following SIV infection in SM. Detection of the initial SIV-specific IFN-γ ELISPOT response in SIVsmE041-infected SM coincided temporally with a decline in peak plasma viremia and was similar in magnitude, specificity, and breadth to SIVsmE041-infected and SIVmac239-infected RM. Despite these similarities, SM showed a greater reduction in postpeak plasma viremia and a more rapid disappearance of productively SIV-infected cells from the lymph node compared with SIVmac239-infected RM. The early Gag-specific CD8$^+$ T lymphocyte response was significantly more polyfunctional in SM compared with RM, and granzyme B-positive CD8$^+$ T lymphocytes were present at significantly higher frequencies in SM even prior to SIV infection. These findings suggest that the early SIV-specific T cell response may be an important determinant of lymphoid tissue viral clearance and absence of lymph node immunopathology in natural hosts of SIV infection. ***The Journal of Immunology*****, 2011, 186: 5151–5161.**

Sooty mangabeys (SM; *Cercocebus atys*) are African Old World primates that are natural hosts of SIV and rarely progress to AIDS despite the presence of ongoing viral replication (1–3). Characteristic differences from pathogenic SIV infection include a lack of aberrant immune activation and preservation of normal lymph node (LN) architecture in chronic SIV infection (1, 3). The mechanisms underlying the lack of immunopathology in SM are not well understood. Studies of experimental SIV infection in SM have shown that similar to pathogenic SIV infection in rhesus macaques (RM), primary SIVsm isolates replicate to peak plasma SIV RNA levels up to 10^7 copies/ml followed by a rapid decline to set-point levels ranging between 10^4 and 10^6 SIV RNA copies/ml (4–7). Although it is widely accepted that the cellular immune response contributes to the containment of primary and chronic viremia in HIV-infected humans and experimentally SIV-infected RM (8–11), its role in natural hosts is less well defined. SIV-specific cellular immune responses are readily detected in SIV-infected SM and African green monkeys (AGM) during chronic SIV infection (12–15). In the setting of primary SIV infection, we previously reported that experimental infection with the macaque-passaged SIVmac239 virus induced a robust SIV-specific CTL response in SM (16, 17). However, SIVmac239 infection was atypical of natural infection because primary viremia was rapidly controlled to near undetectable levels (16). More recently, we showed that in the setting of experimental infection with the primary SIVsm isolate, SIVsmE041, which reproduced the set-point viremia levels seen in natural SIV infection, SM mounted an acute SIV-specific cellular immune response that was comparable in magnitude to RM infected with SIVmac239 or SIVsmE041 (4). In this study, we present a detailed characterization of the primary SIV-specific cellular immune response and its relation to control of viral replication in peripheral blood and lymphoid tissue of experimentally SIV-infected SM and RM.

Kinetic analysis of the cellular immune response in the first 6 mo post-SIV infection showed comparable magnitude, breadth, and specificity of the SIV-specific IFN-γ ELISPOT response in both species. However, SM showed a higher frequency of polyfunctional Gag-specific CD8$^+$ T lymphocytes in the first 10 wk

*Department of Immunology, New England Primate Research Center, Harvard Medical School, Southborough, MA 01772; [†]Department of Comparative Pathology, New England Primate Research Center, Harvard Medical School, Southborough, MA 01772; and [‡]Yerkes National Primate Research Center, Emory University, Atlanta, GA 30322

[1]Current address: Eisai Product Creation Systems, Andover, MA.

[2]Deceased.

[3]Current address: Pfizer Worldwide Research and Development, Andover, MA.

Received for publication December 17, 2010. Accepted for publication March 2, 2011.

This work was supported by Public Health Service Grants RR00168, RR00165, AI49809, and AI46006. Work by the Emory University Center for AIDS Research virology core was supported by Emory Center for AIDS Research Grant P30 AI50409. Reagents were provided by the National Institutes of Health Nonhuman Primate Reagent Resource (Grants R24 RR016001 and N01 AI040101). Custom-conjugated Abs were obtained from the National Institutes of Health Nonhuman Primate Reagent Resource, sponsored by the National Center for Research Resources and National Institutes of Allergy and Infectious Diseases, National Institutes of Health.

Address correspondence and reprint requests to Dr. Amitinder Kaur, Department of Immunology, New England Primate Research Center, Harvard Medical School, One Pine Hill Drive, Southborough, MA 01772. E-mail address: amitinder_kaur@hms.harvard.edu

Abbreviations used in this article: AGM, African green monkey; ISH, in situ hybridization; LN, lymph node; NEPRC, New England Primate Research Center; NIAID, National Institutes of Allergy and Infectious Diseases; NIH, National Institutes of Health; RM, rhesus macaques; SFC, spot-forming cell; SM, sooty mangabeys.

www.jimmunol.org/cgi/doi/10.4049/jimmunol.1004110

following SIV infection, a greater reduction in peak plasma viremia, and a more rapid disappearance of productively SIV-infected cells from the LN compared with SIVmac239-infected RM. These data suggest that qualitative differences in the early SIV-specific cellular immune response might contribute to faster viral load reduction and absence of chronic immunopathology in lymphoid tissues of SIV-infected SM.

Materials and Methods

Animals and SIV infection

SM were housed at the Yerkes National Primate Research Center, Atlanta, GA, whereas RM were housed at the New England Primate Research Center (NEPRC), Southborough, MA. Four SIV-negative SM and 10 SIV-negative RM were enrolled in the current study. All animals were maintained in accordance with institutional and federal guidelines of animal care (18). The primary SM isolate SIVsmE041 and the pathogenic molecular clone SIVmac239 were used for the experimental SIV infection studies as previously described (4). RM were MHC genotyped for the Mamu-A*01, Mamu-B*08, and Mamu-B*17 class I alleles using PCR amplification with allele-specific primers (19).

Sample processing

Samples collected from SM were shipped overnight to NEPRC. Samples collected from RM housed at NEPRC were subjected to a similar overnight delay before processing. Blood collected in CPT vacutainer tubes (Becton Dickinson Vacutainer Systems, Franklin Lakes, NJ) was subjected to centrifugation at 2300 × *g* for 30 min within 1 h of collection for isolation of PBMC prior to shipment. LN lymphocytes were isolated by mechanical dissection and homogenization of biopsy tissue followed by straining through a 70-μm cell strainer (BD Biosciences, San Jose, CA) to remove cell debris. Freshly isolated lymphocytes were used for ELISPOT and immunophenotyping. Viably cryopreserved PBMC were used for flow cytometric evaluation of SIV-specific T lymphocyte responses.

SIV peptides

Fifteen amino acid peptides overlapping by 11 aa and spanning all nine SIV proteins corresponding to the sequence of SIVmac239 were synthesized at the peptide core facility of Massachusetts General Hospital, Charlestown, MA, or were obtained from the AIDS Research and Reference Reagent Program, Division of AIDS, National Institutes of Health (NIH). Individual peptides suspended in 100% DMSO were pooled together for each SIV protein. A total of 10 peptide pools representing Gag, Pol (two pools), Env, Rev, Tat, Nef, Vpr, Vpx, and Vif were used to stimulate PBMC and measure the total SIV-specific response. In some instances, the Vpr, Vpx, and Vif peptides were pooled together. Peptides were used at a final concentration of 1 to 2 μg/ml, with the DMSO concentration being maintained at <0.5% in all functional assays.

Flow cytometry

Polychromatic flow cytometry was used for immunophenotyping and measurement of polyfunctional $CD8^+$ and $CD4^+$ T lymphocytes. Fluorochrome-conjugated mAb of anti-human specificity were obtained from BD Biosciences unless stated otherwise. These included anti-CD3 (clone SP34-2)-Pacific Blue, -PerCP, or -allophycocyanin–Cy7, anti-CD4 (clone L200)-allophycocyanin, -FITC, -PerCP–Cy5.5, anti-CD8 (clone RPA-T8)-Alexa 700, -PE, anti-CD28 (clone CD28.2)-PE, or PE-Texas Red (Beckman Coulter, Fullerton, CA); anti-CD69 (clone FN50)-allophycocyanin–Cy7 or (clone TP1.53.3)–PE-Texas Red (Beckman Coulter); anti-CD95 (clone DX2)–PE-Cy5, -allophycocyanin, biotin, or -PE (Invitrogen, Carlsbad, CA); anti-CCR7 (clone 150503; R&D Systems, Minneapolis, MN)-biotin; anti–Ki-67 (clone B56)-FITC, anti-granzyme B clone GB12-PE, or clone GB11–PE-Texas Red (Invitrogen); anti–IFN-γ (clone 4S.B3)–PE-Cy7, anti–IL-2 (clone MQ1-17H12)-PE or -allophycocyanin, anti–TNF-α (clone MAb11)-allophycocyanin, or -Alexa 700, and anti–MIP-1β (clone 24006)-FITC (R&D Systems). The anti-CD4 (clone L200)-AmCyan or clone (T4/19Thy5D7)-Qdot605 and the anti-CD8 (clone T8/7Pt-3F9)-Qdot 655 mAb were obtained from the NIH Nonhuman Primate Reagent Resource.

The intracellular cytokine stimulation assay was performed as previously described (13, 20). Briefly, 1×10^6 PBMC were incubated in the presence of R-10 medium alone (unstimulated) or SIV Gag peptide pool in the presence of cross-linked anti-CD28 and anti-CD49d costimulatory Abs. Brefeldin A (GolgiPlug; BD Biosciences) was added after 2 h and continued for the remaining period of stimulation. After overnight stimulation, cells were washed and stained for 30 min at 4°C with fluorochrome-conjugated mAbs specific for cell surface molecules. Surface-stained cells were fixed and permeabilized by incubation with Fixation/Permeabilization solution (BD Cytofix/Cytoperm; BD Biosciences) for 20 min at 4°C followed by an incubation with fluorochrome-conjugated anti-CD69 and anti-cytokine mAbs for another 30 min at 4°C. After a final wash, cells were fixed in fresh 2% paraformaldehyde. Samples were run on an LSR II (BD Biosciences) and analyzed by FlowJo software version 8.8.6 (Tree Star, Ashland, OR). Boolean gate analysis was used for analysis of each of 15 possible response patterns based on all possible combinations of four effector functions that were measured. Nonspecific background responses detected in the medium-only control tubes were subtracted from responses in stimulated samples for each of the 15 response patterns using the software Pestle (version 1.6.2 obtained from Mario Roederer, Vaccine Research Center, National Institutes of Allergy and Infectious Diseases [NIAID], NIH). Negative values after background subtraction were set to zero. The software SPICE (version 5.1, courtesy of Mario Roederer and Joshua Nozzi, NIAID, NIH through http://exon.niaid.nih.gov/spice/) was used to analyze polychromatic flow cytometry data and generate graphical representations of T cell responses (21).

ELISPOT assay

IFN-γ ELISPOT assays were performed as previously described (4, 13). The capture- and biotinylated detector-matched mAb pair for IFN-γ were clones GZ-4 and 7-B6-1 (Mabtech, Nack Strand, Sweden), respectively. Briefly, unfractionated PBMC were plated on anti–IFN-γ–coated sterile 96-well polyvinylidene difluoride MultiScreen-IP plates (Millipore, Bedford, MA) and stimulated overnight with SIV peptide pools. Spots were developed by successive incubation with streptavidin-alkaline phosphatase followed by the substrate NBT/5-bromo-4-chloro-3-indolylphosphate buffer (Moss, Pasadena, MD). Spots were counted on a KS ELISPOT Automated Reader System (Carl Zeiss, Thornwood, NY) using KS ELISPOT 4.2 software (performed by ZellNet Consulting, Fort Lee, NJ). Frequencies of responding cells obtained after subtracting background spots in negative control wells were expressed as spot-forming cells (SFC) per million PBMC. ELISPOT responses to individual SIV proteins that were >2-fold above those of negative control wells, and >50 SFC/10^6 cells were considered positive.

Plasma SIV RNA

The concentration of SIV RNA in plasma was determined as previously described (4, 13). Briefly, plasma was separated from blood collected in tubes containing the anticoagulant EDTA within 3 h of collection. Aliquots of twice-spun, cell-free plasma were stored at −80°C. Plasma RNA was extracted with the QIAamp Viral RNA kit (Qiagen, Valentia, CA), and SIV RNA was measured by RT-PCR (7700 Sequence Detection System; PE Applied Biosystems, Carlsbad, CA) using primers and probe targeting a highly conserved region in the 5′ untranslated region (SIVsmE041) or SIV *gag* (SIVmac239). The detection limit of the assays was 160 copies/ml for SIVsmE041 and 30 copies/ml for SIVmac239.

In situ hybridization analysis

Productively infected, SIV-positive cells were identified by in situ hybridization (ISH) for SIV RNA in LN tissue as described previously (4, 22). Digoxigenin-labeled antisense riboprobes (Lofstrand Labs, Gaithersburg, MD) spanning the entire genomes of either SIVsmmFGb or SIVmac239 were used for detection of SIVsmE041- and SIVmac239-infected cells, respectively. After hybridization, sections were washed extensively, and bound probe was detected by immunohistochemistry using alkaline phosphatase-conjugated sheep anti-digoxigenin Fab fragments (Roche, Indianapolis, IN) and the chromogen NBT/5-bromo-4-chloro-3-indolyl-phosphate (Roche). Sections were counterstained with nuclear fast red (Vector Laboratories, Burlingame, CA). The total number of infected cells in all regions of the LN was counted manually and expressed as the number of infected cells per millimeter squared LN area. LN area was quantified using Leica QWin software (Leica Microsystems, Bannockburn, IL), as described elsewhere (22), after image capture on an Optronics DEI-750 charge-coupled device camera (Meyer Instruments, Houston, TX) mounted on an Olympus AH-2 microscope (Olympus America, Center Valley, PA).

Statistical analysis

The nonparametric Mann–Whitney *U* test was used for unpaired comparisons between groups, whereas the nonparametric Wilcoxon matched pairs signed-rank test was used for paired comparisons. All statistical analysis was performed with the GraphPad Prism software version 5.0a (GraphPad Software, La Jolla, CA). The comparison of SIV-specific

T lymphocyte polyfunctionality between groups was determined by the permutation test (SPICE, version 5.1.). The p values <0.05 were considered statistically significant.

Results

Kinetics of plasma viremia in relation to the SIV-specific cellular immune response

Although SIV- and HIV-specific $CD8^+$ T lymphocytes are essential for controlling viral replication in pathogenic lentiviral infection (8–11), their role in maintaining nonpathogenic infection in natural hosts of SIV is uncertain. We recently reported that SIVsmE041-infected SM mounted a SIV-specific cellular immune response during acute infection that is of comparable magnitude to SIVsmE041 and SIVmac239-infected RM (4). In this study, the primary SIV-specific T lymphocyte response and its relation to early control of SIV replication in peripheral blood and lymphoid tissue of SM and RM were evaluated.

Using peptides based on the SIVmac239 sequence, SIV-specific IFN-γ ELISPOT responses toward the entire SIV proteome were evaluated longitudinally in peripheral blood for 6 mo in four SIVsmE041-infected SM (Fig. 1*A*), four SIVsmE041-infected RM (Fig. 1*B*), and six SIVmac239-infected RM (Fig. 1*C*). IFN-γ ELISPOT responses were detected in all animals and temporally coincided with a decline in peak plasma viremia (Fig. 1*A*–*C*). Plasma viremia peaked at 2 to 3 wk and was significantly higher in the SIVmac239-infected RM compared with the SIVsmE041-infected RM and SM (Fig. 2*A*). From week 12 onwards, it was maintained at mean levels of up to 3×10^6 SIV RNA copies/ml in the SIVmac239-infected RM and 1.4×10^4 SIV RNA copies/ml in the SIVsmE041-infected SM (Fig. 2*A*). In contrast, SIVsmE041-infected RM showed a marked decline in plasma SIV RNA levels to near undetectable levels (Figs. 1*B*, 2*A*). The role of the MHC class I alleles Mamu-A*01, Mamu-B*17, and Mamu-B*08 in control of viral replication was examined in the 10 SIV-infected RM. The Mamu-A*01 allele was present in one SIVsmE041-infected RM (111.91) and two SIVmac239-infected RM (112.04 and 330.03, respectively), whereas the Mamu-B*17 and Mamu-B*08 alleles were detected in one RM each (361.95 and 368.05, respectively) in the SIVsmE041 infection group (Fig. 1*B*, 1*C*). Even though three of the four SIVsmE041-infected RM were positive for one of the protective MHC class I alleles, the pattern of SIVsmE041 replication in RM 365.05, which lacked any of these class I alleles, was no different from the other three macaques in this group (Fig. 1*B*). Furthermore, the two SIVmac239-infected Mamu-A*01-positive RM showed a different viral replication pattern compared with the SIVsmE041-infected Mamu-A*01-positive RM (Fig. 1*B*, 1*C*). Overall, these data indicate a viral component to the observed difference in viremia control between the SIVmac239- and SIVsmE041-infected RM.

The kinetics and magnitude of the SIV-specific IFN-γ ELISPOT response in the three monkey groups did not significantly differ from each other in the first 6 mo post-SIV infection (Fig. 2*B*).

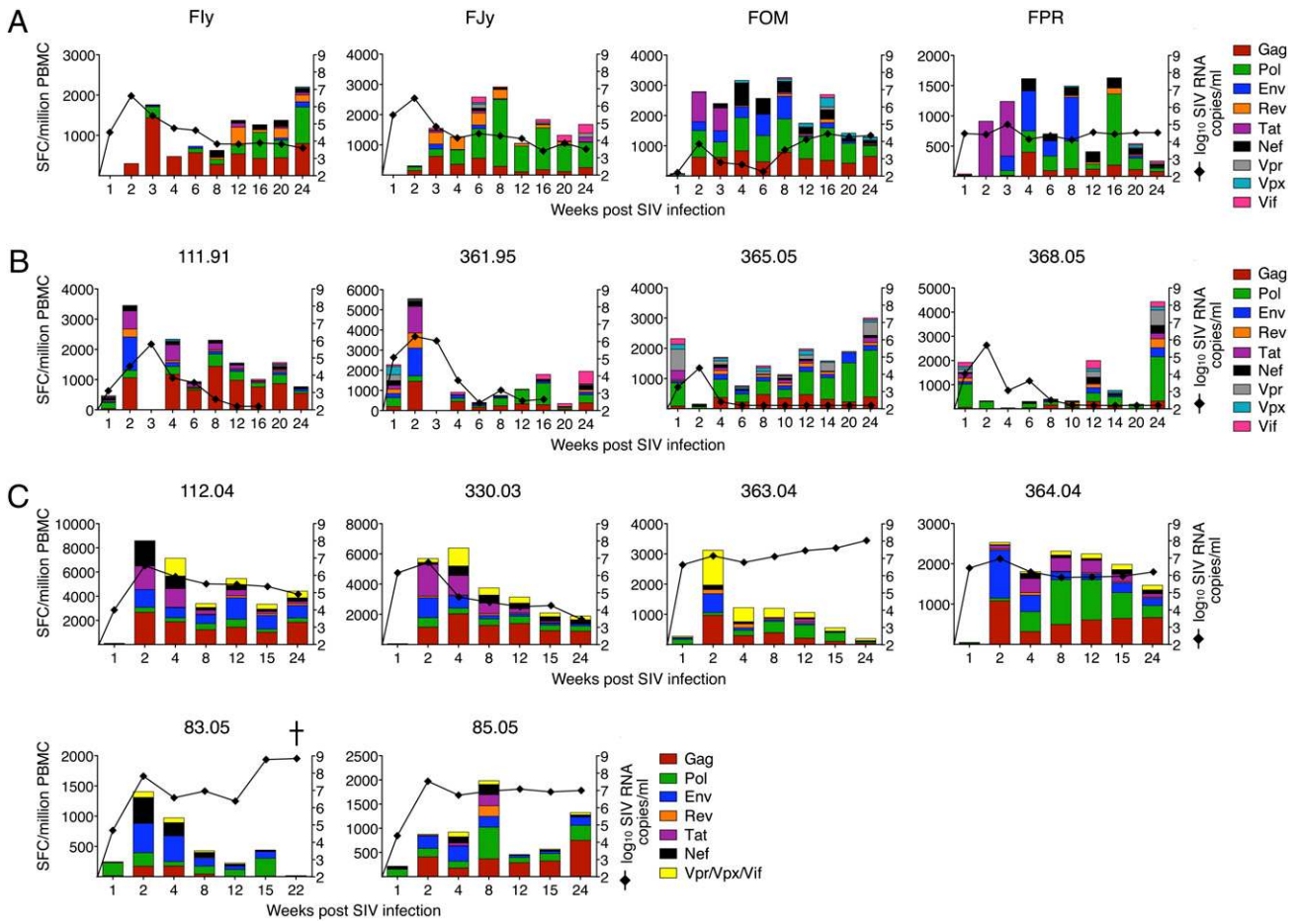

FIGURE 1. Kinetics of the SIV-specific cellular immune response and plasma viremia during acute SIV infection in individual SM and RM. SIV-specific IFN-γ ELISPOT responses and the kinetics of viremia shown in four SIVsmE041-infected SM (*A*), four SIVsmE041-infected RM (*B*), and six SIVmac239-infected RM (*C*). IFN-γ ELISPOT responses expressed as SFC/million PBMC represent values after subtraction of background responses in medium alone wells. Vpr, Vpx, and Vif peptides were pooled into a single well for measurement of IFN-γ ELISPOT responses in SIVmac239-infected RM. Plasma SIV RNA values at wk 20/24 are not available for RM 111.91 and 361.95. †Died of AIDS.

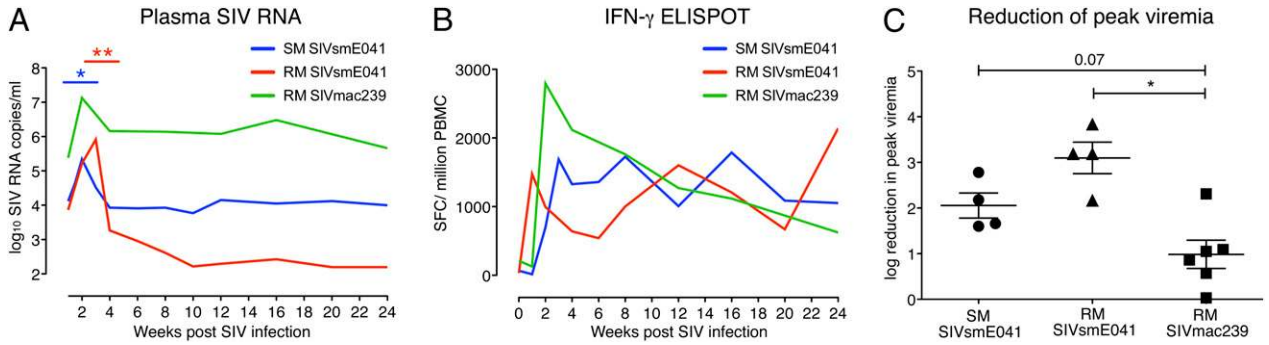

FIGURE 2. Differential reduction in peak plasma SIV viremia in RM and SM. Geometric mean of plasma SIV RNA in SIVsmE041-infected SM (SM SIVsmE041), SIVsmE041-infected RM (RM SIVsmE041), and SIVmac239-infected RM (RM SIVmac239) (*A*). Asterisks (*$p < 0.05$, **$p < 0.01$, Mann–Whitney *U* test) indicate a significant difference in peak viremia of SM SIVsmE041 (blue) or RM SIVsmE041 (red) compared with RM SIVmac239. *B*, Geometric mean of total SIV-specific IFN-γ ELISPOT response in the first 6 mo post-SIV infection. *C*, Comparison of reduction of plasma SIV RNA from peak viremia to week 6–8 post-SIV infection in the three animal groups. Lines denote mean ± SEM. *$p < 0.05$ by Mann–Whitney *U* test.

Despite similarities in the acute SIV-specific cellular immune response, the postpeak reduction in plasma viremia in the SIVsmE041-infected SM and SIVsmE041-infected RM was of greater magnitude compared with the SIVmac239-infected RM (Fig. 2*C*). The difference in magnitude of postpeak reduction between SIVsmE041-infected SM and SIVmac239-infected RM suggests that early control of replication of species-adapted SIV may be better in SM as compared with RM.

Increased effector memory and granzyme B-positive CD8$^+$ T lymphocytes in acute SIV infection

All animals showed an increase in activated Ki-67–positive CD8$^+$ T lymphocytes during the first 4 wk following SIV infection, with the greatest increase occurring in the SIVmac239-infected RM (Fig. 3*A*). By week 24, the frequency of activated CD8$^+$ T lymphocytes had returned to baseline levels in the SM, but persisted at 2–6-fold above baseline levels in the SIVsmE041-infected and SIVmac239-infected RM (Fig. 3*A*). These observations are concordant with published data showing rapid resolution of immune activation in natural hosts following the acute phase of SIV infection (4, 7, 23–25).

Concurrent with the increase in CD8$^+$ T lymphocyte activation, there was an increase in the frequency of circulating granzyme B-positive CD8$^+$ T lymphocytes in SM and RM (Fig. 3*B*). Interestingly, baseline levels of granzyme B-positive CD8$^+$ T lymphocytes in SIV-negative animals were significantly higher in SM compared with RM, and this trend persisted following SIV infection (Fig. 3*C*). This was associated with a significantly higher frequency of effector memory CD8$^+$ T lymphocytes in SM compared with macaques ($p = 0.008$). The age range of SM (6–14 y) and RM (5–19 y) were comparable and did not account for the observed species-specific difference in the frequency of peripheral blood effector memory and granzyme B-positive CD8$^+$ T lymphocytes (data not shown). Following SIV infection, an acute decline in naive (CD95$^-$CD28$^+$) and a corresponding increase in effector memory (CD95$^+$CD28$^-$) CD8$^+$ T lymphocytes were observed in both SM and RM (Fig. 3*D*).

A 2–4-fold increase in Ki-67–positive CD3$^-$CD8$^+$ NK cells was observed in both groups of SIV-infected RM but was much more modest in magnitude in the SIVsmE041-infected SM (Fig. 3*E*). In contrast, an increase in granzyme B-positive NK cells was observed in both RM and SM (Fig. 3*F*).

Specificity and breadth of the cellular immune response during acute SIV infection in RM and SM

The breadth and dominance of the Gag-specific immune response have been associated with lower viral loads and preservation of CD4$^+$ T lymphocyte counts in HIV infection (26–30). We investigated whether differences in the specificity or breadth of the primary cellular immune response might contribute to the differential course of SIV infection in SM and RM.

At its peak, IFN-γ ELISPOT responses against the structural proteins Gag, Pol, and Env were dominant in all three groups and accounted for 56–82% of the total SIV-specific cellular immune response (Fig. 4*A*, Table I). With the exception of Pol- and Tat-specific ELISPOT responses, differences in SIV protein specificity among the three groups were minor during acute SIV infection and did not reach statistical significance (Fig. 4*A*). It is to be noted that the use of SIVmac239-based peptides may have resulted in an underestimation of the SIV-specific T lymphocyte response in the SIVsmE041-infected monkeys. The number of SIV protein pools recognized ranged between two and seven in responding monkeys and did not differ significantly among the three groups of animals (Fig. 4*B*). The LN SIV-specific IFN-γ ELISPOT response in SM and RM also did not significantly differ in magnitude, specificity, or breadth in the first 6 mo post-SIV infection (data not shown).

Early induction of polyfunctional Gag-specific CD8$^+$ T lymphocytes in SM

The functionality of HIV-specific CD8$^+$ T lymphocytes may be an important factor in immune control of HIV infection (31). To determine whether the primary SIV-specific cellular immune response was qualitatively different in SM and RM, we examined its polyfunctionality in acute SIV infection. Cryopreserved PBMC that were available in the first 10 wk post-SIV infection were stimulated with pooled SIV Gag peptides and evaluated for concurrent production of IFN-γ, TNF-α, IL-2, and MIP-1β by polychromatic flow cytometry (Fig. 5*A*).

The total cumulative frequency of Gag-specific memory CD8$^+$ T lymphocytes with four, three, two, and single functionality ranged between 0.13 and 0.21% in the SIVsmE041-infected SM, between 0.17 and 0.41% in the SIVsmE041-infected RM, and between 0.19 and 1.99% in the SIVmac239-infected RM (Table II). Despite the relatively low frequencies, Gag-specific CD8$^+$ T lymphocytes in SM were significantly more polyfunctional compared with SIVmac239-infected RM (Fig. 5*B*). There were no significant differences in functionality of Gag-specific CD4$^+$ T lymphocytes between SM and SIVmac239-infected RM (data not shown). Interestingly, the frequency of SIV-specific CD8$^+$ as compared with CD4$^+$ T lymphocytes was significantly higher in SIVmac239-infected RM ($p = 0.04$) but not in SIVsmE041-infected SM (Table II).

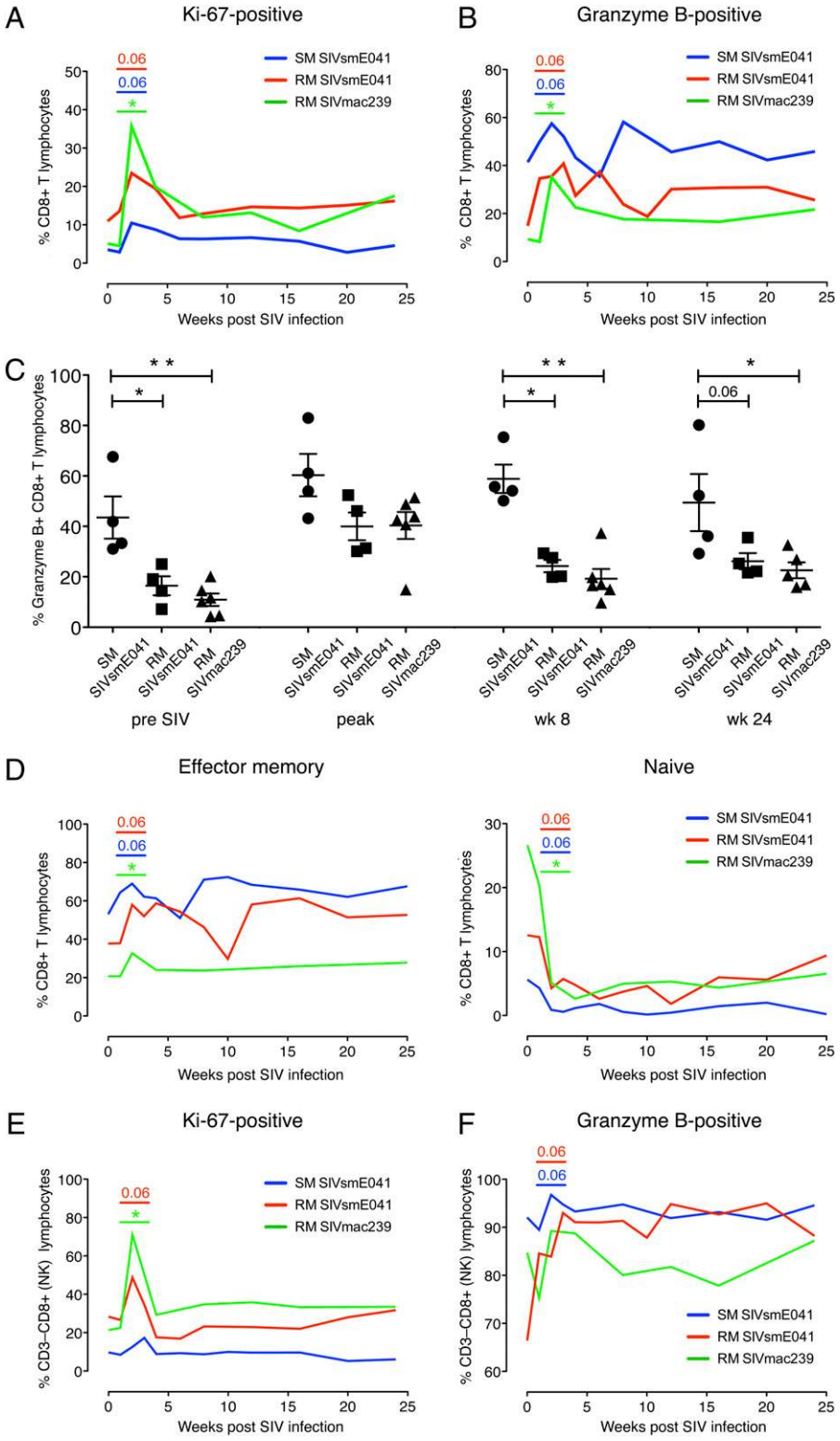

FIGURE 3. Kinetics of $CD8^+$ T and NK lymphocytes during acute SIV infection. Geometric mean frequency of Ki-67–positive $CD8^+$ T lymphocytes (*A*) and granzyme B-positive $CD8^+$ T lymphocytes (*B*) in the first 6 mo post-SIV infection. Asterisks ($*p < 0.01$) indicate significant increases at peak compared with pre-SIV infection levels by the Wilcoxon matched pairs signed-rank test. *C*, Frequency of granzyme B-positive $CD8^+$ T lymphocytes prior to and following SIV infection in each animal group. Lines denote mean ± SEM. Asterisks denote significant differences between groups ($*p < 0.05$, $**p < 0.01$) by the Mann–Whitney *U* test. *D*, Geometric mean frequency of $CD95^+CD28^-$ effector memory and naive $CD95^-CD28^+CD8^+$ T lymphocytes in the first 6 mo post-SIV infection. Asterisks ($*p < 0.05$) indicate a significant change at wk 2–4 from baseline values using the Wilcoxon matched pairs signed-rank test. Geometric mean frequency of Ki-67–positive $CD3^-CD8^+$ NK lymphocytes (*E*) and granzyme B-positive $CD3^-CD8^+$ NK lymphocytes (*F*) in the first 6 mo post-SIV infection. Asterisks ($*p < 0.01$) indicate significant increases at peak compared with pre-SIV infection levels by the Wilcoxon matched pairs signed-rank test.

Rapid disappearance of productively SIV-infected cells from the LN of SM

Disruption of the LN architecture is a hallmark of chronic pathogenic HIV/SIV infection and central to AIDS pathogenesis (32, 33). In contrast, LN of chronically SIV-infected SM show normal architecture and do not have evidence of virus trapping on follicular dendritic cells (1, 3). In this study, we compared the magnitude and clearance kinetics of SIV-infected cells from peripheral LN of SM and RM in primary SIV infection. ISH for SIV RNA revealed productively SIV-infected cells in LN of SIVmac239-infected RM and SIVsmE041-infected SM, but not SIVsmE041-infected RM (Fig. 6*A* and data not shown). Despite the greater than one-log difference in peak plasma viremia levels (Fig. 2*A*), both SIVmac239-infected RM and SIVsmE041-infected SM showed similar numbers of productively SIV-infected cells in the LN at 2 wk post-SIV infection (Fig. 6*A*–*C*). Two main observations were made in terms of: 1) the localization of productively SIV-infected cells; and 2) the kinetics of virus disap-

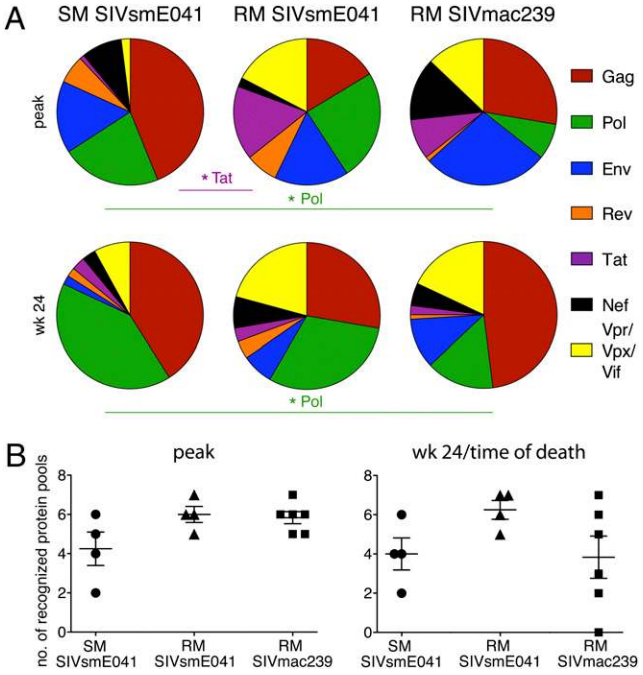

FIGURE 4. Specificity and breadth of the SIV-specific cellular immune response during acute SIV infection. *A*, Pie charts showing the proportion of individual SIV proteins contributing to the total SIV-specific IFN-γ ELISPOT response in the peripheral blood of SIV-infected SM and RM. Mean values for peak (wk 1–4; *upper panels*) and wk 24 (*bottom panels*) shown. *B*, Numbers of recognized proteins at peak and week 24 or time of death post-SIV infection. The regulatory proteins Vpx, Vpr, and Vif have been combined as Vpx/Vpr/Vif for the analysis. Asterisks ($*p < 0.05$, Mann–Whitney *U* test) denote significant differences for individual proteins between groups.

pearance in acute SIV infection. First, although infected cells were present in the paracortex and the germinal centers of the LN in RM, they were confined to the LN paracortex in SM (A.J. Martinot, M. Meythaler, L. Pozzi, K. Boisvert, H. Knight, D. Walsh, S. Westmoreland, A. Kaur, and S.P. O'Neil, manuscript in preparation). Second, although productively SIV-infected cells were still detectable in the LN of four of five SIVmac239-infected RM at 12 wk postinfection, a rapid decline in productively SIV-infected cells was observed in the LN of SM by week 6 post-SIV infection (Fig. 6*A–C*). The difference in virus clearance did not appear to be a result of higher plasma SIV RNA levels in SIVmac239-infected RM because there was no correlation between the numbers of productively SIV-infected cells in the LN and plasma SIV RNA at 2 or 12 wk post-SIV infection (data not shown).

To investigate whether the tissue-localized cellular immune response accounted for the difference in disappearance kinetics of productively SIV-infected cells, we compared the SIV-specific IFN-γ ELISPOT response and granzyme B content in LN of SM and RM at 2, 6, 12, and 20/24 wk post-SIV infection (Fig. 7). Similar to peripheral blood, IFN-γ ELISPOT responses in the LN were detected in all animals at week 2 post-SIV infection. At this time point, the SIV-specific IFN-γ ELISPOT response in the LN of SM was of comparable magnitude to the peripheral blood immune response (Fig. 7*A* and data not shown). In contrast, the SIVmac239-infected RM showed significantly higher SIV-specific IFN-γ ELISPOT responses in the peripheral blood compared with LN at week 2 post-SIV infection (Fig. 7*A*). Consistent with induction of a SIV-specific cellular immune response, both SIVsmE041-infected SM and SIVmac239-infected RM showed a significant and comparable increase in granzyme B-positive $CD8^+$ T lymphocytes in the LN at 2 wk following SIV infection (Fig. 7*B*).

The presence of productively infected cells in the LN germinal center of RM but not SM was not due to differences in location or number of LN $CD8^+$ T lymphocytes in the two species. Immunohistochemical analysis revealed that in both RM and SM, the LN $CD8^+$ T lymphocytes were mainly localized to the paracortical region, with very few being present in the germinal center (data not shown). These findings are consistent with published data on lymphoid tissues in humans (34). We also did not observe any quantifiable difference in the number of paracortical or germinal center $CD8^+$ T lymphocytes between RM and SM either prior to or after SIV infection (data not shown).

Discussion

Early events hold the key to understanding the determinants of pathogenic and nonpathogenic outcome following lentiviral infection. Although the early cellular immune response is central to effective viral control in pathogenic HIV and SIV infection, there are limited data about its efficacy in natural hosts. To our knowledge, we provide the first detailed analysis of the primary cellular immune response against the complete SIV proteome in a natural host of SIV infection and examine early viral control in the peripheral blood and LN of SM and RM in acute SIV infection. The magnitude and specificity of the primary SIV-specific cellular immune response was comparable in SIVsmE041-infected SM, SIVsmE041-infected RM, and SIVmac239-infected RM. However, there were notable differences in the rapidity of early viral control following SIV infection with virus isolates that were either indigenous to their natural host or that had undergone serial passage in their nonnatural host. Thus, SM infected with the primary SIVsm isolate SIVsmE041 showed a greater reduction in peak plasma viremia and a rapid disappearance of productively SIV-infected cells from peripheral lymphoid tissue compared with RM infected with pathogenic SIVmac239. In contrast, RM infected with the non–macaque-passaged SIVsmE041 virus showed a rapid and marked reduction in peak plasma viremia to almost undetectable levels. This virus suppressive effect was recently shown to be due to the presence of an RM TRIM5α genotype that restricts infection by primary SIVsm isolates (35). The kinetics of viral load reduction observed in the blood and LN of SIVsmE041-infected SM was consistent with that observed during primary SIVagm infection of AGM (36).

Table I. Specificity of the SIV-specific IFN-γ ELISPOT response in SM and RM

	SM SIVsmE041							RM SIVsmE041							RM SIVmac239						
Wk Post-SIV	Gag	Pol	Env	Rev	Tat	Nef	V*	Gag	Pol	Env	Rev	Tat	Nef	V*	Gag	Pol	Env	Rev	Tat	Nef	V*
Peak	44	22	16	6	1	9	2	16	24	16	7	16	2	17	28	8	28	1	9	14	13
Wk 12	29	41	0	10	2	16	2	35	36	6	3	3	4	13	32	35	14	1	7	3	8
Wk 24	41	41	2	2	3	3	8	28	31	7	4	3	7	21	48	15	11	1	2	5	18

Values are mean percentages of the total SIV-specific IFN-γ ELISPOT response.
V*, Vpr/Vpx/Vif.

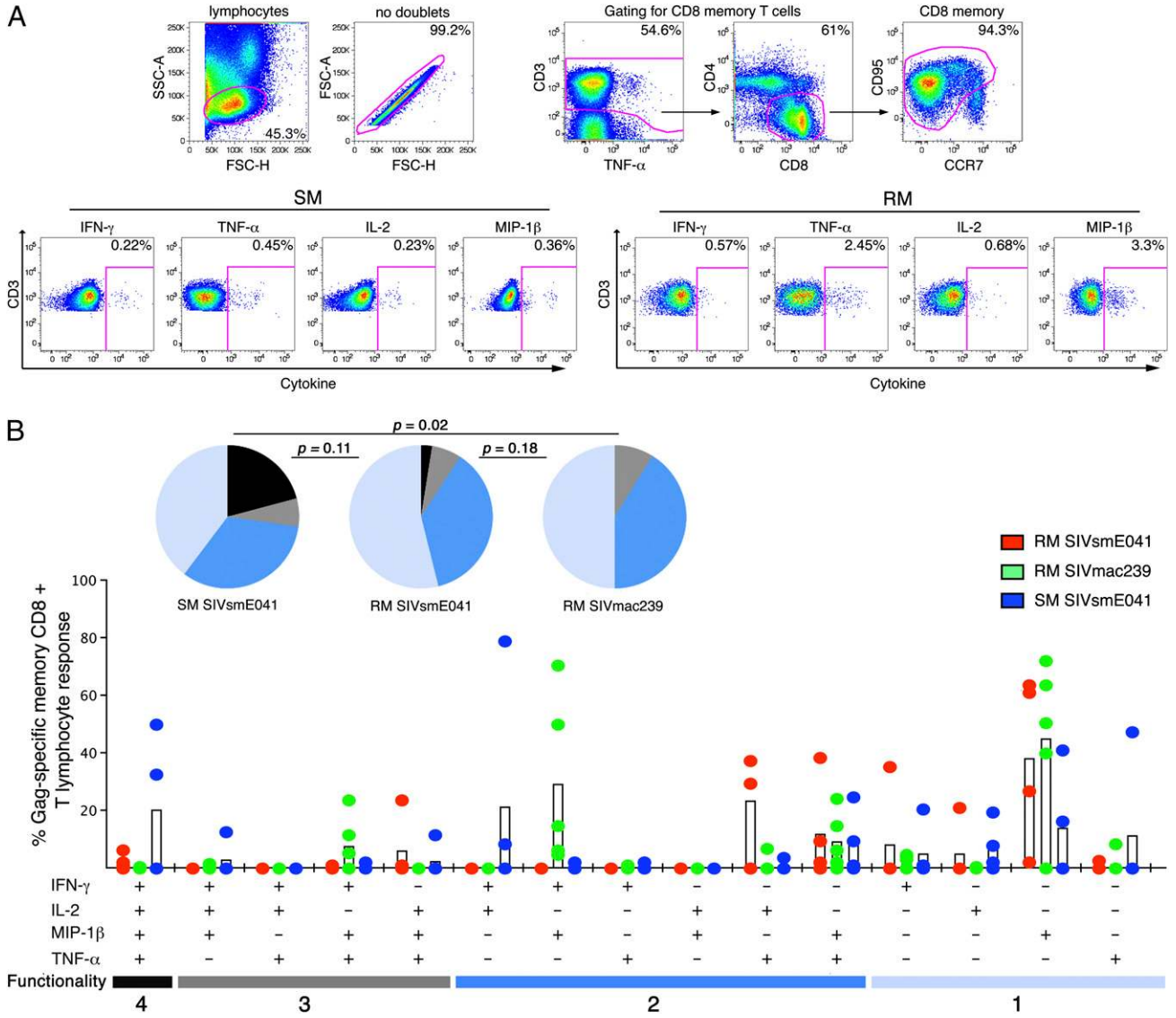

FIGURE 5. Functionality of Gag-specific CD8$^+$ T lymphocytes in SM and RM during acute SIV infection. *A*, Representative dot plots showing gating strategy for the identification of Gag-specific CD8$^+$ T lymphocyte responses. CD4 and CD8 memory T lymphocytes were identified as CD95 positive cells (*upper panel*). The *bottom panel* shows representative plots of cytokine-producing memory CD8$^+$ T lymphocytes in response to Gag peptide stimulation for one SIVsmE041-infected SM (*left panel*) and one SIVsmE041-infected RM (*right panel*) at wk 6 post-SIV infection. *B*, Four-effector function analysis of the Gag-specific CD8$^+$ T lymphocyte response during primary SIV infection in SM and RM using boolean gate analysis. Data at a single time-point in the first 10 wk post-SIV infection shown. The proportion of the total memory CD8$^+$ T lymphocyte response contributed by each cytokine combination for each individual animal (represented by the dots) and the median (represented by the bars) are shown for RM SIVsmE041 (red), RM SIVmac239 (green), and SM SIVsmE041 (blue). The different cytokine combinations are grouped and color-coded by the number of positive functions and summarized in pie charts in which each pie slice represents the mean proportion of the Gag-specific CD8$^+$ T lymphocyte response contributed by cytokine combinations that have all four, three, two, or one of the measured functions. The *p* values were calculated using the permutation test (Spice version 5.1).

In pathogenic HIV and SIV infection, both immune-mediated viral control and target cell restriction have been implicated in the reduction of peak viremia following acute infection. In one study, mathematical modeling of plasma viremia during acute SIV infection in RM showed that the decline in post peak viremia was mainly due to the activity of SIV-specific CD8$^+$ T lymphocytes

Table II. Frequency of Gag-specific memory CD4$^+$ and CD8$^+$ T lymphocytes during acute SIV infection in SM and RM

	Mean Percent (Range)	
	Gag-Specific Memory CD8$^+$ T Lymphocytes	Gag-Specific Memory CD4$^+$ T Lymphocytes
SM SIVsmE041	0.17 (0.13–0.21)	0.46 (0.18–1.04)
RM SIVsmE041	0.28 (0.17–0.41)	0.24 (0.1–0.31)
RM SIVmac239	0.97 (0.19–1.99)	0.33 (0.02–1.28)

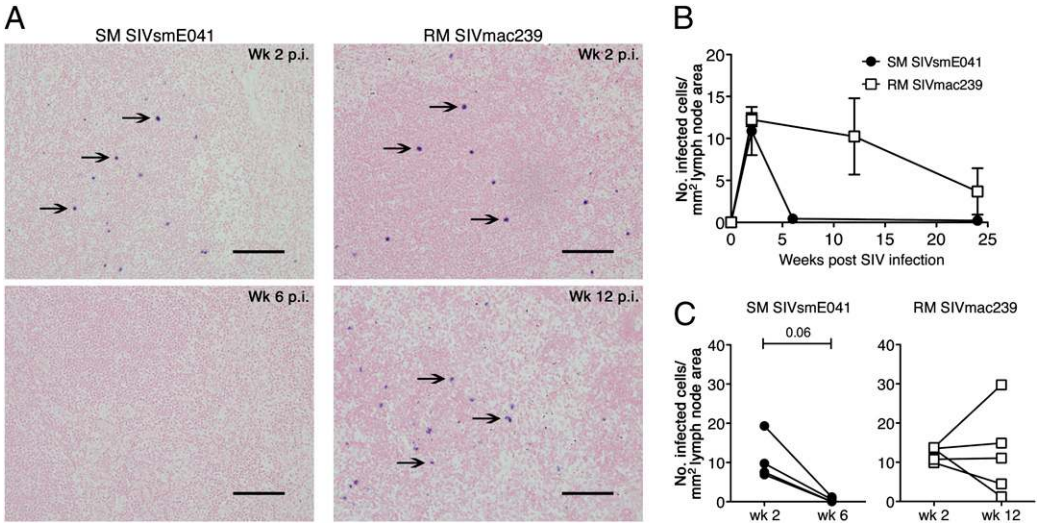

FIGURE 6. Kinetics of LN viral clearance in SM and RM. *A*, Representative SIV RNA ISH to detect productively infected cells (indicated by the arrows) in the peripheral LN of one SIVsmE041-infected SM (*left panels*) and one SIVmac239-infected RM (*right panels*). Scale bars, 100 μm. *B*, Comparison of kinetics of productively SIV-infected cells in the LN in SIVsmE041-infected SM and SIVmac239-infected RM. Mean ± SEM values shown. *C*, LN SIV loads in individual SIVsmE041-infected SM and SIVmac239-infected RM at wk 2 and wk 6/12 post-SIV infection infection. The *p* values calculated using the Wilcoxon matched pairs signed-rank test.

(37). Only limited data are available on the cellular immune response during acute SIV infection in natural hosts. We previously reported that SIVmac239 infection induces a robust SIV-specific CTL response in SM coincident with viremia control of a macaque-passaged SIV isolate (16). However, the low viral load following SIVmac239 infection is not typical of the outcome seen following natural SIV infection in SM. Cellular immune responses against Gag and Env have been reported during acute SIVagm infection in AGM but were not compared with macaque species (38, 39). Detailed comparative analysis of the kinetics of primary viremia and the primary cellular immune response in RM and SM

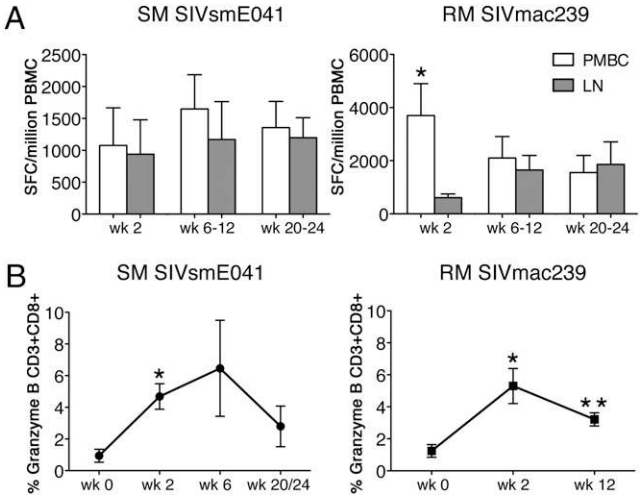

FIGURE 7. LN SIV-specific cellular immune responses in acute SIV infection. *A*, Comparison of SIV-specific immune responses in the peripheral blood versus the LN. Mean ± SEM of the total IFN-γ ELISPOT response shown. Asterisk indicates significant difference (*$p < 0.05$, Wilcoxon matched pairs signed-rank test) between PBMC and LN ELISPOT responses. *B*, Increase in granzyme B-positive $CD8^+$ T lymphocytes in the LN following SIV infection in SIVsmE041-infected SM (*left panel*) and SIVmac239-infected RM (*right panel*). Asterisks (*$p < 0.05$, **$p < 0.01$, Mann–Whitney *U* test) indicate a significant increase above pre-SIV infection levels.

in the current study revealed several similarities in the acute SIV-specific T lymphocyte response between a natural and nonnatural host. The onset of the primary SIV-specific T cell response coincided temporally with a decline in peak plasma viremia in SIVsmE041-infected SM and both SIVsmE041- and SIVmac239-infected RM, suggesting that immune control was a causal factor in the postacute reduction of plasma viremia in both species. In vivo CD8 depletion studies during primary SIV infection in SM (A. Kaur, Z. Wang, N. Kassis, R.M. Ribeiro, S. Pryputniewicz, R.P. Johnson, J. Schmitz, K. Reimann, A.S. Perelson, and S.P. O'Neil, unpublished observations) and AGM (39–41) showed delayed reduction of primary SIV viremia in the absence of $CD8^+$ lymphocytes, providing further evidence that SIV-specific $CD8^+$ T lymphocytes are required for initial control of primary viremia in natural hosts.

Concurrent with the rapid decline in plasma viremia, productively infected cells were undetectable in the LN of SIVsmE041-infected SM by 6 wk post-SIV infection. In contrast, productively infected cells persisted in the LN of four of five SIVmac239-infected macaques at 12 wk post-SIV infection. The difference in clearance of productively infected cells from lymphoid tissue appears to be species-related and not just a manifestation of higher set-point plasma viremia levels in the SIVmac239-infected macaques. Thus, there was no correlation between plasma SIV RNA levels and the number of SIV-infected cells in the LN. At the 2-wk time point when the number of productively infected cells in the LN were comparable in both species, the peak viremia levels in the SIVsmE041-infected mangabeys were at least one-log lower compared with the SIVmac239-infected macaques. In a study comparing SIV-infected cells in the LN of SIVagm-infected AGM and SIVmac251-infected Chinese RM, both species had comparable levels of plasma viremia, and yet AGM showed a greater decline in LN viral load post-SIV infection (42). The persistence of productively infected cells in lymphoid tissue of hosts with pathogenic lentiviral infection has been attributed to inadequate immune clearance due to a variety of factors such as insufficient number of effectors, spatial localization of effectors away from the sites of viral replication, and early induction of immunosuppressive regulatory T lymphocytes (43–45). This raises the intriguing

possibility that the rapid clearance of productively infected cells from the LN of SM may reflect the ability of natural hosts to mount a more effective tissue-localized immune response as opposed to nonnatural hosts (46, 47). In addition to more rapid SIV clearance, SM also showed a striking lack of infected cells in the germinal center of LN. The mechanisms underlying this phenomenon remain unclear. Possibilities include immune-mediated mechanisms, reduced target cell availability, altered SIV tropism, and reduced infection of germinal center $CD4^+$ T lymphocytes due to the absence of trapped SIV on follicular dendritic cells in LN of SM. In the absence of in situ tetramer staining, it is not possible to determine whether, similar to HIV-infected humans (43), species-specific differences in the spatial localization of SIV-specific $CD8^+$ T lymphocytes accounted for the presence or absence of SIV-infected cells in the LN germinal centers.

To address whether host-specific differences in the SIV-specific T lymphocyte response accounted for the greater reduction in postpeak viremia and LN viral clearance in SIVsmE041-infected SM as compared with SIVmac239-infected RM, we evaluated the magnitude and breadth of the total SIV-specific T lymphocyte response by IFN-γ ELISPOT assays over a 6-mo period, and the specificity and quality of the Gag-specific T lymphocyte response at a single time point during acute infection by polychromatic flow cytometry. Similar to chronic SIV infection (4, 13), the total magnitude of the anti-SIV cellular immune response in primary infection did not differ significantly between SIV-infected SM and RM. We compared specificity of the SIV-specific response in the two species because an early Gag-specific immune response was shown to be predictive of a better disease outcome in HIV-infected humans (28, 48). With the exception of Pol- and Tat-specific T cell responses, we did not observe a difference in the specificity or breadth of the SIV proteins targeted by the cellular immune response in the two species. Simultaneous assessment of multiple effector functions by flow cytometry has shown that the quality of the T cell response is an important determinant of protection against several viral infections (49). Virus-specific T lymphocytes that produce more than one cytokine and maintain their proliferative capacity have been implicated in better disease outcome in HIV infection (31, 50–54). In this study, we extended our analysis to evaluate the functionality of SIV-specific T cells in acute infection by polychromatic flow cytometry. Analysis of the Gag-specific response showed induction of both $CD4^+$ and $CD8^+$ T lymphocyte responses in acute infection. However, the Gag-specific response was skewed toward $CD8^+$ T lymphocytes in SIVmac239-infected RM but was more balanced in the SIVsmE041-infected monkeys (Table II). Furthermore, the early Gag-specific $CD8^+$ T lymphocyte response was significantly more polyfunctional in SIVsmE041-infected SM compared with SIVmac239-infected RM (Fig. 5). In light of the lower viremia levels in SIVsmE041-infected SM compared with SIVmac239-infected RM, we cannot exclude the possibility that the increased polyfunctionality in SM was due to a lower Ag load. However, it is noteworthy that the SIVsmE041-infected RM also had low viral loads and yet showed a trend for a less polyfunctional early Gag-specific $CD8^+$ T lymphocyte response compared with the SIVsmE041-infected SM (Fig. 5). Interestingly, the HIV-specific $CD4^+$ and $CD8^+$ T lymphocyte response in the less-pathogenic HIV-2 infection is also characterized by high levels of polyfunctional cells (55). It is tempting to speculate that early induction of polyfunctional SIV-specific T lymphocytes is in part responsible for the better control of postpeak viremia and early clearance of LN viral load in SIV-infected SM. In addition to immune control, other factors such as target cell availability could also be contributing to low viral loads in the LN of SIV-infected SM. The recent report of SM homozygous for defective CCR5 alleles has raised the possibility that altered coreceptor usage could alter the in vivo tropism of SIVsm in SIV-infected SM (56).

In addition to the functional response to SIV peptides, we also used granzyme B as a surrogate marker for CTL activity. We observed that this cohort of SM had significantly higher baseline levels of granzyme B and effector memory $CD8^+$ T lymphocytes as compared with RM. This difference was age-independent and persisted even after SIV infection. A recent study also reported higher granzyme B levels in $CD8^+$ T lymphocytes in SIV-negative AGM as compared with SIV-negative RM (15), suggesting that this observation is not unique to SM and may be common to other natural hosts of SIV infection. The significance of the high granzyme B content of $CD8^+$ T lymphocytes in SM and AGM remains unclear. It is possible that the higher frequency of effector memory granzyme B-positive $CD8^+$ T lymphocytes in SM translates to more efficient killing of virus-infected cells, which in turn could to lead to better control of viremia without inducing aberrant immune activation. This situation may be akin to the efficient lytic granule loading capacity of HIV-specific $CD8^+$ T lymphocytes in elite controllers (57, 58), albeit with partial viral control in natural hosts.

In summary, the analysis of the primary SIV-specific cellular immune response and viral kinetics in this study has highlighted key similarities in the adaptive immune response mounted by natural and nonnatural hosts of SIV infection and shown differences in viral control, particularly at the level of lymphoid tissue. It is possible that differences in the quality and location of the early immune response in natural hosts might prevent LN damage and set the stage for lack of disease progression during chronic infection.

Acknowledgments

We thank Preston Marx (Tulane National Primate Research Center) for the primary SM isolate SIVsmE041, Ron Desrosiers (NEPRC) for the pathogenic clone SIVmac239, Michael Piatak, Jr. and Jeffrey Lifson (Science Applications International Corp. Frederick AIDS vaccine program) for the determination of the SIVmac239 viral loads, and the Emory University Center for AIDS Research virology core for the SIVsmE041 RNA measurements. SIV peptides were obtained through the AIDS Research and Reference Reagent Program, Division of AIDS, NIAID, NIH. The software SPICE: A Data Mining and Visualization Software for Multicolor Flow Cytometry was developed by Mario Roederer and Joshua Nozzi and was accessed through http://exon.niaid.nih.gov/spice/. The software Pestle was kindly provided by Mario Roederer, Vaccine Research Center, NIH.

Disclosures

The authors have no financial conflicts of interest.

References

1. Rey-Cuillé, M. A., J. L. Berthier, M. C. Bomsel-Demontoy, Y. Chaduc, L. Montagnier, A. G. Hovanessian, and L. A. Chakrabarti. 1998. Simian immunodeficiency virus replicates to high levels in sooty mangabeys without inducing disease. *J. Virol.* 72: 3872–3886.
2. Ling, B., C. Apetrei, I. Pandrea, R. S. Veazey, A. A. Lackner, B. Gormus, and P. A. Marx. 2004. Classic AIDS in a sooty mangabey after an 18-year natural infection. *J. Virol.* 78: 8902–8908.
3. Silvestri, G., D. L. Sodora, R. A. Koup, M. Paiardini, S. P. O'Neil, H. M. McClure, S. I. Staprans, and M. B. Feinberg. 2003. Nonpathogenic SIV infection of sooty mangabeys is characterized by limited bystander immunopathology despite chronic high-level viremia. *Immunity* 18: 441–452.
4. Meythaler, M., A. Martinot, Z. Wang, S. Pryputniewicz, M. Kasheta, B. Ling, P. A. Marx, S. O'Neil, and A. Kaur. 2009. Differential CD4+ T-lymphocyte apoptosis and bystander T-cell activation in rhesus macaques and sooty mangabeys during acute simian immunodeficiency virus infection. *J. Virol.* 83: 572–583.
5. Gordon, S. N., N. R. Klatt, S. E. Bosinger, J. M. Brenchley, J. M. Milush, J. C. Engram, R. M. Dunham, M. Paiardini, S. Klucking, A. Danesh, et al. 2007. Severe depletion of mucosal CD4+ T cells in AIDS-free simian immunodeficiency virus-infected sooty mangabeys. *J. Immunol.* 179: 3026–3034.

6. Silvestri, G., A. Fedanov, S. Germon, N. Kozyr, W. J. Kaiser, D. A. Garber, H. McClure, M. B. Feinberg, and S. I. Staprans. 2005. Divergent host responses during primary simian immunodeficiency virus SIVsm infection of natural sooty mangabey and nonnatural rhesus macaque hosts. *J. Virol.* 79: 4043–4054.
7. Estes, J. D., S. N. Gordon, M. Zeng, A. M. Chahroudi, R. M. Dunham, S. I. Staprans, C. S. Reilly, G. Silvestri, and A. T. Haase. 2008. Early resolution of acute immune activation and induction of PD-1 in SIV-infected sooty mangabeys distinguishes nonpathogenic from pathogenic infection in rhesus macaques. *J. Immunol.* 180: 6798–6807.
8. Koup, R. A., J. T. Safrit, Y. Cao, C. A. Andrews, G. McLeod, W. Borkowsky, C. Farthing, and D. D. Ho. 1994. Temporal association of cellular immune responses with the initial control of viremia in primary human immunodeficiency virus type 1 syndrome. *J. Virol.* 68: 4650–4655.
9. Matano, T., R. Shibata, C. Siemon, M. Connors, H. C. Lane, and M. A. Martin. 1998. Administration of an anti-CD8 monoclonal antibody interferes with the clearance of chimeric simian/human immunodeficiency virus during primary infections of rhesus macaques. *J. Virol.* 72: 164–169.
10. Jin, X., D. E. Bauer, S. E. Tuttleton, S. Lewin, A. Gettie, J. Blanchard, C. E. Irwin, J. T. Safrit, J. Mittler, L. Weinberger, et al. 1999. Dramatic rise in plasma viremia after CD8(+) T cell depletion in simian immunodeficiency virus-infected macaques. *J. Exp. Med.* 189: 991–998.
11. Schmitz, J. E., M. J. Kuroda, S. Santra, V. G. Sasseville, M. A. Simon, M. A. Lifton, P. Racz, K. Tenner-Racz, M. Dalesandro, B. J. Scallon, et al. 1999. Control of viremia in simian immunodeficiency virus infection by CD8+ lymphocytes. *Science* 283: 857–860.
12. Kaur, A., J. Yang, D. Hempel, L. Gritz, G. P. Mazzara, H. McClure, and R. P. Johnson. 2000. Identification of multiple simian immunodeficiency virus (SIV)-specific CTL epitopes in sooty mangabeys with natural and experimentally acquired SIV infection. *J. Immunol.* 164: 934–943.
13. Wang, Z., B. Metcalf, R. M. Ribeiro, H. McClure, and A. Kaur. 2006. Th-1-type cytotoxic CD8+ T-lymphocyte responses to simian immunodeficiency virus (SIV) are a consistent feature of natural SIV infection in sooty mangabeys. *J. Virol.* 80: 2771–2783.
14. Dunham, R., P. Pagliardini, S. Gordon, B. Sumpter, J. Engram, A. Moanna, M. Paiardini, J. N. Mandl, B. Lawson, S. Garg, et al. 2006. The AIDS resistance of naturally SIV-infected sooty mangabeys is independent of cellular immunity to the virus. *Blood* 108: 209–217.
15. Zahn, R. C., M. D. Rett, B. Korioth-Schmitz, Y. Sun, A. P. Buzby, S. Goldstein, C. R. Brown, R. A. Byrum, G. J. Freeman, N. L. Letvin, et al. 2008. Simian immunodeficiency virus (SIV)-specific CD8+ T-cell responses in vervet African green monkeys chronically infected with SIVagm. *J. Virol.* 82: 11577–11588.
16. Kaur, A., R. M. Grant, R. E. Means, H. McClure, M. Feinberg, and R. P. Johnson. 1998. Diverse host responses and outcomes following simian immunodeficiency virus SIVmac239 infection in sooty mangabeys and rhesus macaques. *J. Virol.* 72: 9597–9611.
17. Kaur, A., L. Alexander, S. I. Staprans, L. Denekamp, C. L. Hale, H. M. McClure, M. B. Feinberg, R. C. Desrosiers, and R. P. Johnson. 2001. Emergence of cytotoxic T lymphocyte escape mutations in nonpathogenic simian immunodeficiency virus infection. *Eur. J. Immunol.* 31: 3207–3217.
18. Anonymous. 1996. *Guide for Care and Use of Laboratory Animals.* Institute of Laboratory Animal Resources, National Council, Washington, D.C., p. 86–123.
19. Kaizu, M., G. J. Borchardt, C. E. Glidden, D. L. Fisk, J. T. Loffredo, D. I. Watkins, and W. M. Rehrauer. 2007. Molecular typing of major histocompatibility complex class I alleles in the Indian rhesus macaque which restrict SIV CD8+ T cell epitopes. *Immunogenetics* 59: 693–703.
20. Kaur, A., C. L. Hale, B. Noren, N. Kassis, M. A. Simon, and R. P. Johnson. 2002. Decreased frequency of cytomegalovirus (CMV)-specific CD4+ T lymphocytes in simian immunodeficiency virus-infected rhesus macaques: inverse relationship with CMV viremia. *J. Virol.* 76: 3646–3658.
21. Roederer, M., J. L. Nozzi, and M. C. Nason. 2011. SPICE: exploration and analysis of post-cytometric complex multivariate datasets. *Cytometry A* 79: 167–174.
22. O'Neil, S. P., C. Suwyn, D. C. Anderson, G. Niedziela, J. Bradley, F. J. Novembre, J. G. Herndon, and H. M. McClure. 2004. Correlation of acute humoral response with brain virus burden and survival time in pig-tailed macaques infected with the neurovirulent simian immunodeficiency virus SIVsmmFGb. *Am. J. Pathol.* 164: 1157–1172.
23. Jacquelin, B., V. Mayau, B. Targat, A. S. Liovat, D. Kunkel, G. Petitjean, M. A. Dillies, P. Roques, C. Butor, G. Silvestri, et al. 2009. Nonpathogenic SIV infection of African green monkeys induces a strong but rapidly controlled type I IFN response. *J. Clin. Invest.* 119: 3544–3555.
24. Bosinger, S. E., Q. Li, S. N. Gordon, N. R. Klatt, L. Duan, L. Xu, N. Francella, A. Sidahmed, A. J. Smith, E. M. Cramer, et al. 2009. Global genomic analysis reveals rapid control of a robust innate response in SIV-infected sooty mangabeys. *J. Clin. Invest.* 119: 3556–3572.
25. Harris, L. D., B. Tabb, D. L. Sodora, M. Paiardini, N. R. Klatt, D. C. Douek, G. Silvestri, M. Müller-Trutwin, I. Vasile-Pandrea, C. Apetrei, et al. 2010. Downregulation of robust acute type I interferon responses distinguishes nonpathogenic simian immunodeficiency virus (SIV) infection of natural hosts from pathogenic SIV infection of rhesus macaques. *J. Virol.* 84: 7886–7891.
26. Zuñiga, R., A. Lucchetti, P. Galvan, S. Sanchez, C. Sanchez, A. Hernandez, H. Sanchez, N. Frahm, C. H. Linde, H. S. Hewitt, et al. 2006. Relative dominance of Gag p24-specific cytotoxic T lymphocytes is associated with human immunodeficiency virus control. *J. Virol.* 80: 3122–3125.
27. Masemola, A., T. Mashishi, G. Khoury, P. Mohube, P. Mokgotho, E. Vardas, M. Colvin, L. Zijenah, D. Katzenstein, R. Musonda, et al; HIVNET 028 Study Team. 2004. Hierarchical targeting of subtype C human immunodeficiency virus type 1 proteins by CD8+ T cells: correlation with viral load. *J. Virol.* 78: 3233–3243.
28. Peretz, Y., C. M. Tsoukas, and N. F. Bernard. 2008. HIV Gag-specific immune responses predict the rate of CD4 decline. *AIDS* 22: 1222–1224.
29. Kiepiela, P., K. Ngumbela, C. Thobakgale, D. Ramduth, I. Honeyborne, E. Moodley, S. Reddy, C. de Pierres, Z. Mncube, N. Mkhwanazi, et al. 2007. CD8+ T-cell responses to different HIV proteins have discordant associations with viral load. *Nat. Med.* 13: 46–53.
30. Honeyborne, I., A. Prendergast, F. Pereyra, A. Leslie, H. Crawford, R. Payne, S. Reddy, K. Bishop, E. Moodley, K. Nair, et al. 2007. Control of human immunodeficiency virus type 1 is associated with HLA-B*13 and targeting of multiple gag-specific CD8+ T-cell epitopes. *J. Virol.* 81: 3667–3672.
31. Betts, M. R., M. C. Nason, S. M. West, S. C. De Rosa, S. A. Migueles, J. Abraham, M. M. Lederman, J. M. Benito, P. A. Goepfert, M. Connors, et al. 2006. HIV nonprogressors preferentially maintain highly functional HIV-specific CD8+ T cells. *Blood* 107: 4781–4789.
32. Fauci, A. S. 1993. Immunopathogenesis of HIV infection. *J. Acquir. Immune Defic. Syndr.* 6: 655–662.
33. Pantaleo, G., C. Graziosi, and A. S. Fauci. 1993. The role of lymphoid organs in the pathogenesis of HIV infection. *Semin. Immunol.* 5: 157–163.
34. Folkvord, J. M., C. Armon, and E. Connick. 2005. Lymphoid follicles are sites of heightened human immunodeficiency virus type 1 (HIV-1) replication and reduced antiretroviral effector mechanisms. *AIDS Res. Hum. Retroviruses* 21: 363–370.
35. Kirmaier, A., F. Wu, R. M. Newman, L. R. Hall, J. S. Morgan, S. O'Connor, P. A. Marx, M. Meythaler, S. Goldstein, A. Buckler-White, et al. 2010. TRIM5 suppresses cross-species transmission of a primate immunodeficiency virus and selects for emergence of resistant variants in the new species. *PLoS Biol.* 8: e1000462.
36. Diop, O. M., A. Gueye, M. Dias-Tavares, C. Kornfeld, A. Faye, P. Ave, M. Huerre, S. Corbet, F. Barre-Sinoussi, and M. C. Müller-Trutwin. 2000. High levels of viral replication during primary simian immunodeficiency virus SIVagm infection are rapidly and strongly controlled in African green monkeys. *J. Virol.* 74: 7538–7547.
37. Regoes, R. R., R. Antia, D. A. Garber, G. Silvestri, M. B. Feinberg, and S. I. Staprans. 2004. Roles of target cells and virus-specific cellular immunity in primary simian immunodeficiency virus infection. *J. Virol.* 78: 4866–4875.
38. Lozano Reina, J. M., D. Favre, Z. Kasakow, V. Mayau, M. T. Nugeyre, T. Ka, A. Faye, C. J. Miller, D. Scott-Algara, J. M. McCune, et al. 2009. Gag p27-specific B- and T-cell responses in Simian immunodeficiency virus SIVagm-infected African green monkeys. *J. Virol.* 83: 2770–2777.
39. Zahn, R. C., M. D. Rett, M. Li, H. Tang, B. Korioth-Schmitz, H. Balachandran, R. White, S. Pryputniewicz, N. L. Letvin, A. Kaur, et al. 2010. Suppression of adaptive immune responses during primary SIV infection of sabaeus African green monkeys delays partial containment of viremia but does not induce disease. *Blood* 115: 3070–3078.
40. Schmitz, J. E., R. C. Zahn, C. R. Brown, M. D. Rett, M. Li, H. Tang, S. Pryputniewicz, R. A. Byrum, A. Kaur, D. C. Montefiori, et al. 2009. Inhibition of adaptive immune responses leads to a fatal clinical outcome in SIV-infected pigtailed macaques but not vervet African green monkeys. *PLoS Pathog.* 5: e1000691.
41. Gaufin, T., R. M. Ribeiro, R. Gautam, J. Dufour, D. Mandell, C. Apetrei, and I. Pandrea. 2010. Experimental depletion of CD8+ cells in acutely SIVagm-infected African Green Monkeys results in increased viral replication. *Retrovirology* 7: 42.
42. Cumont, M. C., O. Diop, B. Vaslin, C. Elbim, L. Viollet, V. Monceaux, S. Lay, G. Silvestri, R. Le Grand, M. Müller-Trutwin, et al. 2008. Early divergence in lymphoid tissue apoptosis between pathogenic and nonpathogenic simian immunodeficiency virus infections of nonhuman primates. *J. Virol.* 82: 1175–1184.
43. Connick, E., T. Mattila, J. M. Folkvord, R. Schlichtemeier, A. L. Meditz, M. G. Ray, M. D. McCarter, S. Mawhinney, A. Hage, C. White, and P. J. Skinner. 2007. CTL fail to accumulate at sites of HIV-1 replication in lymphoid tissue. *J. Immunol.* 178: 6975–6983.
44. Estes, J. D., Q. Li, M. R. Reynolds, S. Wietgrefe, L. Duan, T. Schacker, L. J. Picker, D. I. Watkins, J. D. Lifson, C. Reilly, et al. 2006. Premature induction of an immunosuppressive regulatory T cell response during acute simian immunodeficiency virus infection. *J. Infect. Dis.* 193: 703–712.
45. Li, Q., P. J. Skinner, S. J. Ha, L. Duan, T. L. Mattila, A. Hage, C. White, D. L. Barber, L. O'Mara, P. J. Southern, et al. 2009. Visualizing antigen-specific and infected cells in situ predicts outcomes in early viral infection. *Science* 323: 1726–1729.
46. Kuroda, M. J., J. E. Schmitz, W. A. Charini, C. E. Nickerson, M. A. Lifton, C. I. Lord, M. A. Forman, and N. L. Letvin. 1999. Emergence of CTL coincides with clearance of virus during primary simian immunodeficiency virus infection in rhesus monkeys. *J. Immunol.* 162: 5127–5133.
47. Pantaleo, G., H. Soudeyns, J. F. Demarest, M. Vaccarezza, C. Graziosi, S. Paolucci, M. B. Daucher, O. J. Cohen, F. Denis, W. E. Biddison, et al. 1997. Accumulation of human immunodeficiency virus-specific cytotoxic T lymphocytes away from the predominant site of virus replication during primary infection. *Eur. J. Immunol.* 27: 3166–3173.
48. Edwards, B. H., A. Bansal, S. Sabbaj, J. Bakari, M. J. Mulligan, and P. A. Goepfert. 2002. Magnitude of functional CD8+ T-cell responses to the gag protein of human immunodeficiency virus type 1 correlates inversely with viral load in plasma. *J. Virol.* 76: 2298–2305.
49. Seder, R. A., P. A. Darrah, and M. Roederer. 2008. T-cell quality in memory and protection: implications for vaccine design. *Nat. Rev. Immunol.* 8: 247–258.
50. Julg, B., K. L. Williams, S. Reddy, K. Bishop, Y. Qi, M. Carrington, P. J. Goulder, T. Ndung'u, and B. D. Walker. 2010. Enhanced anti-HIV

functional activity associated with Gag-specific CD8 T-cell responses. *J. Virol.* 84: 5540–5549.
51. Brenchley, J. M., K. S. Knox, A. I. Asher, D. A. Price, L. M. Kohli, E. Gostick, B. J. Hill, C. A. Hage, Z. Brahmi, A. Khoruts, et al. 2008. High frequencies of polyfunctional HIV-specific T cells are associated with preservation of mucosal CD4 T cells in bronchoalveolar lavage. *Mucosal Immunol.* 1: 49–58.
52. Ferre, A. L., P. W. Hunt, J. W. Critchfield, D. H. Young, M. M. Morris, J. C. Garcia, R. B. Pollard, H. F. Yee, Jr., J. N. Martin, S. G. Deeks, and B. L. Shacklett. 2009. Mucosal immune responses to HIV-1 in elite controllers: a potential correlate of immune control. *Blood* 113: 3978–3989.
53. Owen, R. E., J. W. Heitman, D. F. Hirschkorn, M. C. Lanteri, H. H. Biswas, J. N. Martin, M. R. Krone, S. G. Deeks, P. J. Norris; NIAID Center for HIV/AIDS Vaccine Immunology. 2010. HIV+ elite controllers have low HIV-specific T-cell activation yet maintain strong, polyfunctional T-cell responses. *AIDS* 24: 1095–1105.
54. Migueles, S. A., A. C. Laborico, W. L. Shupert, M. S. Sabbaghian, R. Rabin, C. W. Hallahan, D. Van Baarle, S. Kostense, F. Miedema, M. McLaughlin, et al. 2002. HIV-specific CD8+ T cell proliferation is coupled to perforin expression and is maintained in nonprogressors. *Nat. Immunol.* 3: 1061–1068.
55. Duvall, M. G., M. L. Precopio, D. A. Ambrozak, A. Jaye, A. J. McMichael, H. C. Whittle, M. Roederer, S. L. Rowland-Jones, and R. A. Koup. 2008. Polyfunctional T cell responses are a hallmark of HIV-2 infection. *Eur. J. Immunol.* 38: 350–363.
56. Riddick, N. E., E. A. Hermann, L. M. Loftin, S. T. Elliott, W. C. Wey, B. Cervasi, J. Taaffe, J. C. Engram, B. Li, J. G. Else, et al. 2010. A novel CCR5 mutation common in sooty mangabeys reveals SIVsmm infection of CCR5-null natural hosts and efficient alternative coreceptor use in vivo. *PLoS Pathog.* 6: e1001064.
57. Migueles, S. A., C. M. Osborne, C. Royce, A. A. Compton, R. P. Joshi, K. A. Weeks, J. E. Rood, A. M. Berkley, J. B. Sacha, N. A. Cogliano-Shutta, et al. 2008. Lytic granule loading of CD8+ T cells is required for HIV-infected cell elimination associated with immune control. *Immunity* 29: 1009–1021.
58. Hersperger, A. R., F. Pereyra, M. Nason, K. Demers, P. Sheth, L. Y. Shin, C. M. Kovacs, B. Rodriguez, S. F. Sieg, L. Teixeira-Johnson, et al. 2010. Perforin expression directly ex vivo by HIV-specific CD8 T-cells is a correlate of HIV elite control. *PLoS Pathog.* 6: e1000917.